

# BEAM DYNAMICS STUDIES WITH NON-NEUTRAL PLASMA TRAPS\*

H. Okamoto<sup>#</sup>, K. Fukushima, H. Higaki, D. Ishikawa, K. Ito, T. Iwai, K. Moriya, T. Okano, K. Osaki, M. Yamaguchi, AdSM, Hiroshima University, Higashi-Hiroshima 739-8530, Japan

## Abstract

Compact non-neutral plasma traps have been developed at Hiroshima University to explore fundamental aspects of space-charge-dominated beam dynamics. The whole experimental system is referred to as “S-POD” (Simulator of Particle Orbit Dynamics) composed mainly of either a linear Paul trap or a magnetic Penning trap, DC and AC power sources, a vacuum system, several plasma diagnostic tools (Faraday cup, CCD camera, MCP with a phosphor screen), and a personal computer that controls a sequence of measurements without human intervention to retune parameters. Five independent S-POD systems are currently operational, three of which employ Paul traps and the other two employ Penning traps. This novel accelerator-free experiment is based on an isomorphism between non-neutral plasmas in the traps and charged-particle beams traveling in a periodic AG focusing channel. S-POD has been applied for various beam dynamics studies including the intensity and lattice-structure dependence of coherent resonance instability, stop-band crossing in non-scaling FFAg accelerators, mismatch-induced halo formation, etc. This paper gives a brief summary of recent experimental results from S-POD.

## INTRODUCTION

The idea of using non-neutral plasma traps for beam physics purposes was proposed over a decade ago [1,2]. After that, the S-POD systems were constructed at Hiroshima University to study various fundamental issues in modern particle accelerators [3]. As theoretically explained in Ref. [1], either a linear Paul trap or a Penning trap can provide a many-body Coulomb system very similar to a charged-particle beam focused by linear external forces. This physical analogy gives us a

possibility of answering some important beam dynamics questions without relying on large-scale machines.

The linear Paul trap currently utilized for resonance crossing experiments is shown in Fig. 1. Other Paul traps also have a similar structure. Four electrodes are symmetrically placed to generate a radio-frequency (rf) quadrupole field for transverse ion confinement [4]. They are axially divided into five electrically isolated pieces, so that we can add DC bias voltages to form a longitudinal potential well as illustrated in Fig. 2 [5]. The axial length of the trap is only about 20 cm. The aperture size is 1 cm in diameter. A different type of linear Paul trap was designed in Princeton Plasma Physics Laboratory, which had been used for beam physics experiments until recently [6,7].

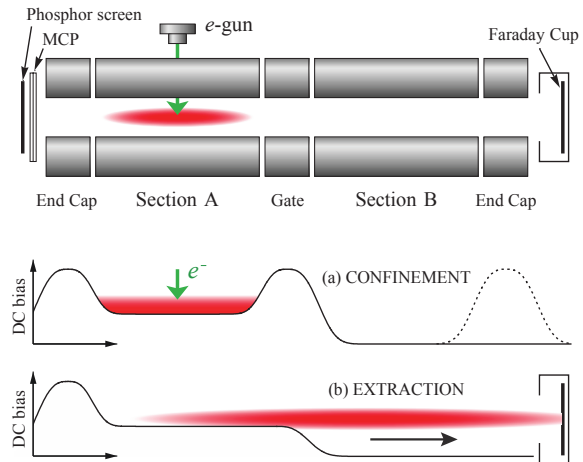


Figure 2: Typical measurement steps.

The transverse motion of ions confined in an ordinary linear Paul trap is governed by the Hamiltonian [1]

$$H = \frac{p_x^2 + p_y^2}{2} + \frac{1}{2} K_{rf}(\tau)(x^2 - y^2) + I\phi, \quad (1)$$

where the independent variable is  $\tau = ct$  with  $c$  being the speed of light,  $K_{rf}(\tau)$  is proportional to the rf voltage applied to the quadrupole rods,  $I$  is a constant depending on the ion species, and  $\phi$  is the collective Coulomb potential that satisfies the Poisson equation. This is just identical to the well-known betatron Hamiltonian of an intense beam traveling in a linear AG transport channel. Since the phase-space distribution function of confined particles obeys the Vlasov equation in both cases (beams and non-neutral plasmas), these two dynamical systems are physically equivalent; namely, what happens in a plasma trap should also happen in a beam transport. As

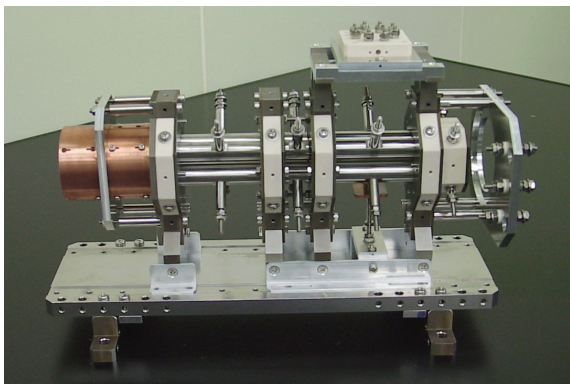


Figure 1 : A multi-sectioned Paul trap for S-POD.

\*Work supported in part by a Grant-in-Aid for Scientific Research, Japan Society for Promotion of Science.  
<sup>#</sup>okamoto@sci.hiroshima-u.ac.jp

Content from this work may be used under the terms of the CC BY 3.0 licence (© 2014). Any distribution of this work must maintain attribution to the author(s), title of the work, publisher, and DOI.

discussed later, we can introduce periodic dipole kicks, if necessary, to emulate the effect of dipole imperfections in a circular accelerator\*.

In the following, we try to summarize recent output from the S-POD systems. The next few chapters are devoted to describing typical Paul-trap experiments. Emphasis is placed upon resonant ion losses depending on plasma intensity and rf focusing waveforms. We then briefly discuss preliminary results of Penning-trap experiments performed to investigate halo formation caused by a strong initial disturbance to the plasma.

## EXPERIMENT METHOD

Among several reasonable choices of ion species for a Paul trap, we have picked  $^{40}\text{Ar}^+$  in most experiments so far.  $^{40}\text{Ar}^+$  ions are generated by ionizing neutral Ar gases with a low energy electron beam from an  $e$ -gun. The generated ions are confined in Section A (see Fig. 2) above which the  $e$ -gun is located. The plasma density can be controlled to some degree by changing the ionization period, the Ar-gas pressure, and the  $e$ -beam current. In case  $^{40}\text{Ca}^+$  ions are chosen instead of  $^{40}\text{Ar}^+$ , the Doppler cooling technique becomes available, which makes it possible to achieve the ultimate full-range control of the plasma density in phase space. The operating rf frequency is usually set at 1 MHz with the most popular sinusoidal waveform. The rf amplitude required to survey the whole tune space is only less than 100 V for  $^{40}\text{Ar}^+$  or  $^{40}\text{Ca}^+$ .

After a proper number of ions are trapped, we switch off the  $e$ -gun and, then, keep the plasma in Section A for a certain period of time, manipulating the plasma-confinement condition to look into a particular effect of interest. For instance, to observe the ion-loss behaviour during resonance stop-band crossing, we ramp the amplitude of the rf quadrupole voltage over a certain range within a certain period. As soon as a specific plasma manipulation process is completed, the DC bias voltage on the Gate electrode (or the End Cap) is dropped to send the plasma toward the Faraday cup (or the MCP) as sketched in Fig. 2(b). It only takes a few seconds to finish a single measurement process even if a beam transport over thousands of AG focusing cells are experimentally simulated. Needless to say, we have absolutely no problem losing all charged particles in an instant due to any plasma instabilities intentionally excited for beam dynamics studies.

## STOP BAND MEASUREMENTS

A major advantage of S-POD experiment is the controllability of external AG focusing patterns. In a real machine, the lattice structure cannot be changed after the construction. We thus need another machine to study any dynamic behaviour of a beam focused by an essentially different AG lattice. In contrast, the time variation of the

external linear focusing force to charged particles in a Paul trap is determined by the waveform of the rf voltages applied to the quadrupole electrodes. Therefore, we can experimentally simulate beam dynamics in arbitrary quadrupole lattice structures simply by changing the rf waveform [8,9]. In this section, we address recent S-POD results on resonant beam instability expected in a few standard lattice structures, namely, doublet, triplet, and FFDD. In these experiments,  $^{40}\text{Ar}^+$  plasmas are confined for 10 ms in Section A (see Fig. 2) with the rf waveform corresponding to a specific lattice structure of interest. Ions surviving after the 10-ms storage are eventually detected either by the Faraday cup or the MCP on the other side. The detected ion number is significantly reduced in the event of any instability. Since the operating rf frequency is 1 MHz, 10 ms corresponds to 10,000 AG focusing periods. It is not an issue at all to extend the storage period by an order of magnitude.

### Beam Intensity Dependence

First of all, let us consider the so-called ‘‘FODO’’ lattice where two quadrupoles having the same length and same field gradient (but opposite signs) are equidistantly placed. The horizontal and vertical *bare* phase advances,  $\sigma_{0x}$  and  $\sigma_{0y}$ , respectively, are equal in this case, namely,  $\sigma_{0x} = \sigma_{0y} (\equiv \sigma_0)$ . Figure 3 shows the results of four separate S-POD experiments performed with four different initial ion numbers. Each line contains 260 points of independent measurements carried out at 260 different values of  $\sigma_0$ . The process of 260 consecutive measurements is completely automated and takes only about 40 minutes. From these data, we confirm the existence of three major stop bands slightly above the bare phase advances of 60, 90, and 120 degrees, all of which move rightward as the initial plasma intensity increases. This ion-loss behaviour depending on  $\sigma_0$  and plasma intensity can be explained fairly well by the one-dimensional sheet-beam model [10] that concludes the following resonance condition:

$$\sigma_0 - C_m \Delta\sigma \approx 360^\circ \times \left( \frac{n}{2m} \right), \quad (2)$$

where  $\Delta\sigma$  represents the shift of the design bare phase advance originating from the Coulomb repulsion,  $m$  is the order of a collective oscillation mode,  $C_m$  is a  $m$ -dependent constant less than unity, and  $n$  is an integer. An analogous condition was first derived by Sacherer while the factor 1/2 on the right hand side is missing in his formula [11]. According to Eq. (2), the  $m = 2$  mode (the lowest-order linear mode) should be responsible for the serious ion losses near  $\sigma_0 = 90$  degrees when the plasma density is high<sup>†</sup>. The ion losses near  $\sigma_0 = 60$  and 120 degrees are caused mainly by the third-order ( $m = 3$ )

\* Note that in a Paul trap the dipole kick is not magnetic but electric. The kick strength is thus independent of particle velocities, which means that we cannot reproduce the effect of momentum dispersion in the rf trap.

<sup>†</sup> At low density, the error-induced fourth-order ( $m=4$ ) instability, rather than the linear collective resonance, plays a more important role in ion losses near  $\sigma_0 = 90$  degrees.

Content from this work may be used under the terms of the CC BY 3.0 licence (© 2014). Any distribution of this work must maintain attribution to the author(s), title of the work, publisher, and DOI.

instability. In particular, the stop band near  $\sigma_0 = 60$  degrees is almost purely due to a space-charge-driven resonance, which means that the ion losses become negligible at low plasma density.

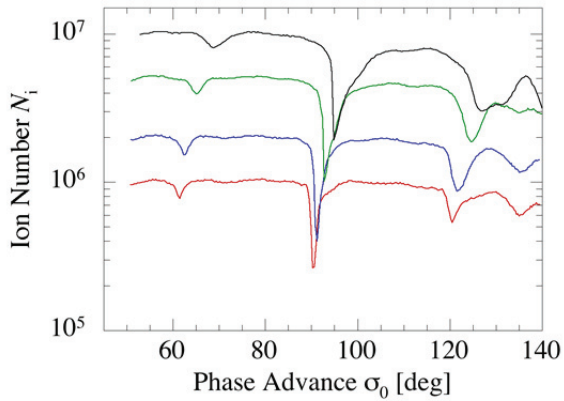


Figure 3: Stop bands in FODO focusing.

### Lattice Structure Dependence

We recently conducted systematic measurements of stop bands in general *doublet* focusing, varying the quadrupole occupancy factor and the ratio of drift spaces. Doublets are more or less similar to the FODO channel and, in fact, we always observed the three stop bands in Fig. 3, regardless of the details of the rf-pulse configurations; the stop-band distributions turned out to be quite insensitive to the change of the geometric factors.

It is also straightforward in S-POD to break the symmetric focusing condition  $\sigma_{0x} = \sigma_{0y}$ ; all we have to do is just making the focusing and defocusing pulse widths different. By adjusting the widths of the two pulses in a doublet cell, we can experimentally survey the transverse tune space as demonstrated in Fig. 4. The initial number of ions has been set at  $10^7$  in this example where the plasma should be in the space-charge-dominant regime. We observe clear resonance lines associated with the linear ( $m = 2$ ) and nonlinear ( $m = 3$ ) instabilities in both horizontal and vertical betatron motions.

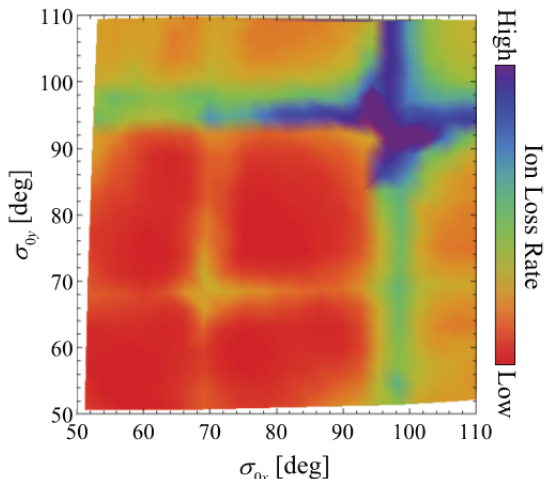


Figure 4: Tune diagram of doublet focusing.

All resonance lines have been remarkably shifted to the higher  $\sigma_0$  side. The size of these stop-bands' shifts suggests that the tune depression at this plasma intensity is roughly around 0.9.

Another popular AG focusing structure is the *triplet* consisting of three consecutive quadrupoles, the first and third of which provide defocusing (focusing) and the central quad focusing (defocusing). As an example, we here consider a symmetric triplet where the first and third pulses with the same height are equidistant from the central. If we change  $\sigma_{0y}$  over a wide range while keeping the geometric factors,  $\sigma_{0x}$  varies as indicated in Fig. 5. The corresponding stop-band distribution plotted as a function of  $\sigma_{0y}$  is given in Fig. 6. Since  $\sigma_{0x} \neq \sigma_{0y}$ , the low-order stop bands have split, which makes the distribution a bit more complex than the FODO case in Fig. 3. Nevertheless, the observed ion losses can still be explained by Eq. (2) with  $m = 2$  or 3 if we replace  $\sigma_0$  either by  $\sigma_{0x}$  or  $\sigma_{0y}$ .

We are now working on an AG lattice with double focusing plus double defocusing (FFDD). Such a lattice structure has been employed, e.g., for UNILAC at GSI [12] and CERN PS [13]. The latest results from S-POD have supported the natural expectation that the stop-band distribution of the FFDD lattice should be similar to the doublet case.

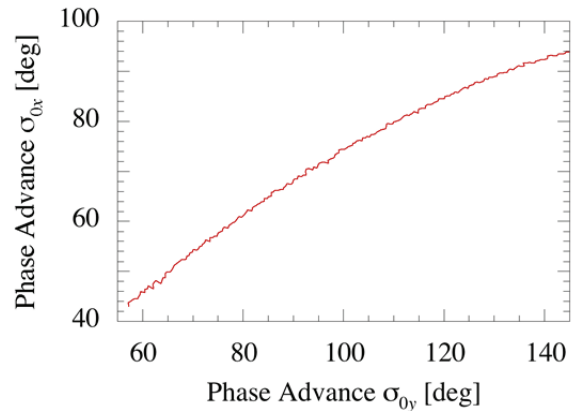


Figure 5: Relation between the horizontal and vertical phase advances in the triplet lattice assumed here.

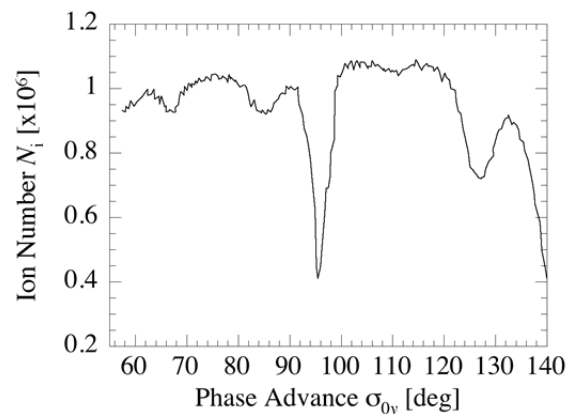


Figure 6: Stop bands in triplet focusing.

## RESONANCE CROSSING

The operating bare tunes of a circular machine are usually fixed at certain numbers that guarantee the beam stability. In some exceptional cases, however, the effective operating point inevitably moves on the tune diagram. Such unique situations take place, e.g., in cooler storage rings (where the effective tunes may be depressed strongly by the space-charge potential) and in non-scaling FFAG accelerators. In the latter case, the operating tune

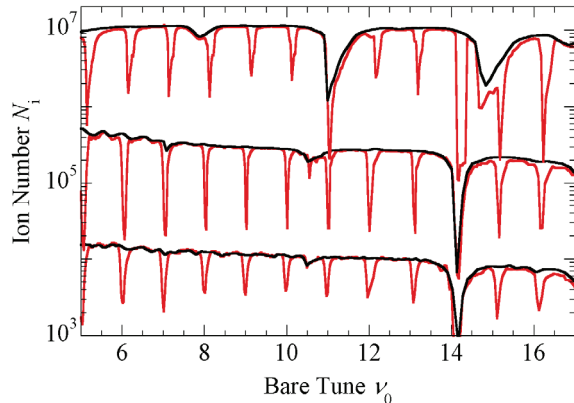


Figure 7: Stop bands with (red) and without (black) a pulsed dipole perturbation.

quickly decreases during beam acceleration, traversing many resonance stop bands. In S-POD, we can readily move the operating point either upward or downward over an arbitrary range at various speeds. Comprehensive S-POD experiments and numerical simulations were done to estimate possible ion losses when the operating point crosses the three major stop bands of low-order modes identified in Fig. 3 [14]. We have reached the conclusion that in a high beam-density regime, crossing the space-charge-driven linear resonance at  $\sigma_0 \approx 90$  degrees gives rise to particularly severe ion losses.

In the ns-FFAG “EMMA” constructed in England [15], crossing of the integer-resonance stop bands excited by dipole leakage fields from the septum magnets has become an important issue [16]. Linear Paul traps are generally free from integer resonances because of the symmetric excitation of the quadrupole electrodes. A dipole perturbation can, however, be introduced very easily by applying weak rf voltages of opposite signs to two horizontal or vertical electrodes facing each other [16]. Figure 7 shows the stop-band distributions with and without a dipole perturbation, measured at three different initial ion numbers. Considering the EMMA situation, we have assumed a ring composed of 42 FODO cells. The abscissa represents the transverse bare tune around the ring. The width and height of the dipole kick applied to the plasma every 42 rf focusing periods are fixed at  $1 \mu\text{s}$  and  $0.5 \text{ V}$ , respectively. In addition to the linear ( $m = 2$ ) and nonlinear ( $m = 3$ ) stop bands near the bare tunes  $\nu_0 = 42/6$ ,  $42/4$ , and  $42/3$ , the dipole instability has occurred at every integer tune. We recognize that unlike the  $m = 2$  and  $m = 3$  resonances, the dipole resonance is

independent of the plasma density. A number of systematic measurements were recently performed under the condition that the operating point traverses one or two adjacent integer stop bands [17,18]. It was pointed out that nonlinear error fields have noticeable effect on ion losses at integer stop bands especially when the dipole perturbation is weak. We also experimentally verified that in double resonance crossing, the dipole oscillation excited at the first stop band is not necessarily enhanced at the second stop band but can rather be suppressed depending on the timing of the second integer crossing.

## HALO FORMATION

Unlike the experiments reported in the above sections, the Penning traps, instead of the Paul traps, have been employed for the study of mismatch-induced halo formation. The magnetic S-POD system based on a Penning trap enables us to explore the collective motion of a simple, rotationally symmetric beam focused by a continuous harmonic potential [1]. In the halo formation experiment, we usually reduce the field strength below 100 G to lower the Brillouin density limit. This makes it easier for us to increase the plasma density in phase space, while the plasma lifetime is considerably shortened. We have so far used pure electron plasmas rather than ions that require a much higher field for stable transverse confinement. Inside the solenoid coil, there are many ring-shaped electrodes aligned along the trap axis, which are DC biased to provide an axial potential well. We first remove the potential barrier on the particle-source ( $e$ -gun) side, keep injecting electrons for a while, and finally reconstruct the barrier by switching the DC bias on. The electron plasma trapped in this way probably has a rather strong initial mismatch that could be a source of halo formation. It is possible to intentionally apply a mismatch to the plasma, if necessary, by quickly changing the axial potential depth. We recently confirmed that a clear halo is formed even without such an intentional mismatch; in other words, the present electron injection and trapping scheme already gives a serious disturbance to the confined plasma as expected.

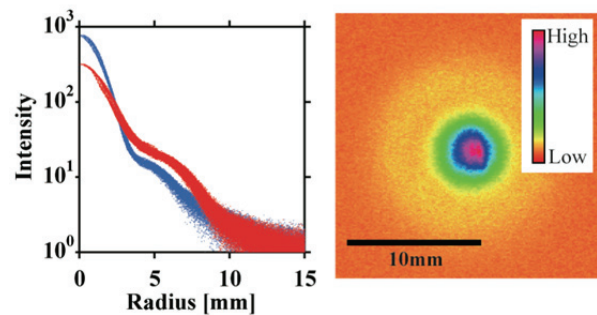


Figure 8: Transverse profiles of an electron plasma at the beginning and after a 7-ms storage in the Penning trap. The axial field strength is fixed at 64G. (Left) the initial (blue) and final (red) electron distributions, (Right) the final transverse profile observed on the phosphor screen.

Figure 8 is the typical transverse profiles of an electron plasma confined in the Penning trap for 7 ms, then extracted and measured with a CCD camera. In this example, we did not apply any intentional mismatch to the plasma but just keep it in the constant external potential, expecting the natural collective relaxation of the electron distribution toward a sort of equilibrium state. The blue and red lines in the left panel show, respectively, the initial plasma profile and the final observed after 7 ms. The phosphor image of the final transverse profile is shown in the right panel. Preliminary experimental data suggest that a few collective-mode oscillations are enhanced after a certain period of the plasma relaxation, leading to halo formation. We presently suspect that the longitudinal and transverse temperatures of the plasma core are gradually reduced during the relaxation process and, at some point, a low-order collective mode becomes resonantly unstable. Multi-particle PIC simulations indicate that the longitudinal plasma temperature should be an important factor in understanding this phenomenon. Systematic Penning-trap experiments are now in progress to clarify the fundamental mechanism.

## CONCLUDING REMARKS

Since the first proposal of the application of compact non-neutral plasma traps for beam dynamics studies [1], we have designed, constructed, and improved the S-POD systems at Hiroshima University. This novel, accelerator-free experiment allows quick evaluation of various nonlinear beam instabilities whose accurate study is often troublesome in practice. S-POD should be particularly useful in exploring space-charge-induced collective effects even though it has some technical limitations. We have run several independent S-POD systems side by side to understand the conditions of coherent betatron resonances depending on AG lattice structures and beam intensities, resonance crossing effects in ns-FFAGs, halo formation from intense mismatched hadron beams, etc. Other fundamental beam-physics issues are also within the scope of S-POD experiments, such as longitudinal dynamics including synchrotron resonances, space-charge effects in short bunches, beam cooling and related collective instabilities at ultralow temperature, etc.

Two of the S-POD systems are equipped with a Doppler laser cooler for  $^{40}\text{Ca}^+$  ions, which could considerably widen the range of S-POD experiments. The Doppler cooling technique, in principle, enables us to produce an ion plasma that has an arbitrary density in phase space, in other words, any tune depression is achievable with this technique. Since we can condition the initial state of a plasma with the powerful cooling force, it is probably possible to extend the plasma lifetime, which is very convenient for the systematic study of long-term space-charge effects. The use of  $^{40}\text{Ca}^+$  plasmas is advantageous from a diagnostic point of view as well, because laser-induced fluorescence signals are available for high-resolution, real-time plasma monitoring. For the production of  $^{40}\text{Ca}^+$  ions, however, we

must turn on an atomic oven. Increasing the Ca-gas pressure is, therefore, practically more problematic than the preparation of neutral Ar gases (For instance, too strong a jet of hot Ca atoms from the oven may seriously contaminate the electrode surfaces, distorting the plasma confinement potential.). In order to confine  $^{40}\text{Ca}^+$  ions as many as or even more than  $^{40}\text{Ar}^+$  ions in previous S-POD experiments, we are now trying to establish the *plasma stacking scheme* discussed in Ref. [5]. According to preliminary experiments recently done, we can actually increase the number of  $^{40}\text{Ca}^+$  ions by accumulating them in Section B of the Paul trap (see Fig. 2) with the cooling laser on. Careful optimization of some parameters such as the laser-frequency detuning and the DC bias on Section A will hopefully enhance the initial intensity of  $^{40}\text{Ca}^+$  plasmas at least up to the level presently attained with  $^{40}\text{Ar}^+$  ions.

## ACKNOWLEDGMENTS

The authors would like to thank Drs. S. Sheehy, D. Kelliher, S. Machida, and C. Prior for valuable discussion and information on the ns-FFAG “EMMA”. They are also indebted to Dr. S. M. Lund for his assistance in doing numerical simulations. One of the authors (HO) expresses his sincere gratitude to Dr. A. M. Sessler for his support during the course of this work.

## REFERENCES

- [1] H. Okamoto, H. Tanaka, Nucl. Instrum. Meth. A 437, 178 (1999).
- [2] H. Okamoto, Y. Wada, R. Takai, Nucl. Instrum. Meth. A 485, 244, (2002).
- [3] H. Okamoto, et al., Nucl. Instrum. Meth. A 733, 119, (2014).
- [4] P. K. Ghosh, “Ion Traps” and references therein, Oxford Science, Oxford, (1995).
- [5] R. Takai, et al., Jpn. J. Appl. Phys. 45, 5332, (2006).
- [6] R. C. Davidson, H. Qin, G. Shvets, Phys. Plasma 7, 1020, (2000).
- [7] E. Gilson, et al., Phys. Rev. Lett. 92, 155002, (2004).
- [8] S. Ohtsubo, et al., Phys. Rev. ST Accel. Beams 13, 044201, (2010).
- [9] K. Fukushima, et al., Nucl. Instrum. Meth. A 733, 18, (2014).
- [10] H. Okamoto, K. Yokoya, Nucl. Instrum. Meth. A 482, 51, (2002).
- [11] F. J. Sacherer, Ph.D thesis, Lawrence Radiation Laboratory [Report No. UCRL-18454, 1968].
- [12] L. Groening, et al., Phys. Rev. Lett. 102, 234801, (2009).
- [13] S. Machida, private communication.
- [14] H. Takeuchi, et al., Phys. Rev. ST Accel. Beams 15, 074201, (2012).
- [15] S. Machida, et al., Nature Physics 8, 243, (2012).
- [16] S. L. Sheehy, et al., WEPEA072, IPAC’13, Shanghai, May 2013, p. 2675, (2013).
- [17] D. Kelliher, et al., TUPRI009, IPAC’14, Dresden, Germany, (2014).